

# Learning Patch-to-Cluster Attention in Vision Transformer

Ryan Grainger<sup>†</sup>, Thomas Paniagua<sup>†</sup>, Xi Song<sup>‡</sup> and Tianfu Wu<sup>†\*</sup>

<sup>†</sup>Department of Electrical and Computer Engineering, North Carolina State University, USA

<sup>‡</sup>An Independent Researcher

{rpgraing, tapaniag, twu19}@ncsu.edu, xsong.lhi@gmail.com

## Abstract

*The Vision Transformer (ViT) model is built on the assumption of treating image patches as “visual tokens” and learning patch-to-patch attention. The patch embedding based tokenizer is a workaround in practice and has a semantic gap with respect to its counterpart, the textual tokenizer. The patch-to-patch attention suffers from the quadratic complexity issue, and also makes it non-trivial to explain learned ViT models. To address these issues in ViT models, this paper proposes to learn patch-to-cluster attention (PaCa) based ViT models. Queries in our PaCa-ViT are based on patches, while keys and values are based on clustering (with a predefined small number of clusters). The clusters are learned end-to-end, leading to better tokenizers and realizing joint clustering-for-attention and attention-for-clustering when deployed in ViT models. The quadratic complexity is relaxed to linear complexity. Also, directly visualizing the learned clusters can reveal how a trained ViT model learns to perform a task (e.g., object detection). In experiments, the proposed PaCa-ViT is tested on CIFAR-100 and ImageNet-1000 image classification, and MS-COCO object detection and instance segmentation. Compared with prior arts, it obtains better performance in classification and comparable performance in detection and segmentation. It is significantly more efficient in COCO due to the linear complexity. The learned clusters are also semantically meaningful and shed light on designing more discriminative yet interpretable ViT models.*

## 1. Introduction

A picture is worth a thousand words. Seeking solutions that can bridge the semantic gap between those words and raw image data has long been, and remains, a grand challenge in computer vision, machine learning and AI. Deep learning has revolutionized the field of computer vision in the past decade. More recently, the Vision Transformer

(ViT) model [12, 40] has witnessed remarkable progress in computer vision. ViT is built on the assumption of treating image patches as “visual tokens” using patch embedding and learns patch-to-patch attention. Unlike the textual tokens provided as inputs in natural language processing, visual tokens need to be learned first and continuously refined for more effective learning of ViT models. The patch embedding based tokenizer is a workaround in practice and has a semantic gap with respect to its counterpart, the textual tokenizer. On one hand, due to the well-known issue of the quadratic complexity of vanilla Transformer models and the 2D spatial nature of images (Fig. 1 and Eqn. 1), it is a non-trivial task of developing ViT models that are applicable for many vision problems including image classification, object detection and semantic segmentation. On the other hand, explaining trained ViT models requires non-trivial and sophisticated methods [6] following the trend of eXplainable AI (XAI) [18] that has been extensively studied with convolutional neural networks.

To address the quadratic complexity, there have been two main variants developed very recently with great success obtained: One is to exploit the vanilla Transformer model locally using a predefined window size (e.g.,  $7 \times 7$ ) such as the Swin-Transformer [27] (Fig. 2 (a)) and the nested variant of ViT [57]. The other is to exploit another patch embedding at a coarser level (i.e., nested patch embedding, Fig. 2 (b)) to reduce the sequence length before computing the keys and values (while keeping the query length unchanged) [43, 44, 48]. Most of these variants follow the patch-to-patch attention setup used in the vanilla ViT models [12]. Meanwhile, most Transformer explanation methods are post-hoc and focus on the vanilla ViT models in image classification [6]. And, explaining ViT models for downstream tasks such as object detection and instance segmentation has not been studied well.

Although existing ViT variants have shown great results in practice, patch embedding based approaches may not be the best way of learning visual tokens due to the underlying predefined subsampling of the image lattice. Additionally, patch-to-patch embedding does not account for the

\*T. Wu is the corresponding author.

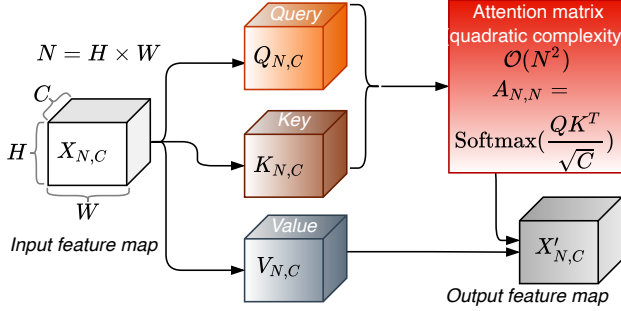


Figure 1. The quadratic complexity of the vanilla ViT models [12, 40]. It hinders its isotropic applicability in vision tasks that entail retaining high-resolution feature maps. The input sequence  $X_{N,C}$  of  $N$  “tokens” is flattened from an input feature map  $X_{H,W,C}$  with the height and width ( $H, W$ ) and  $N = H \times W$ . See text for details.

spatial redundancy due to the compositional nature of images and reusable parts in images [17]. Thus, it is worth exploring alternative methods towards learning more semantically meaningful visual tokens. A question arises naturally: *Can we rethink the patch-to-patch attention mechanism in vision tasks to hit three birds (reducing complexity, facilitating better visual tokenizer and enabling simple forward explainability) with one stone?*

As shown in Fig. 3, this paper proposes to learn **Patch-to-Cluster Attention (PaCa)** under the stage-wise pyramidal architecture of assembling Vision Transformer [43, 44]. The proposed PaCa module is a straightforward way to address the aforementioned challenge: Given an input sequence  $X_{N,C}$ , a light-weight clustering module finds meaningful clusters by computing  $\mathcal{C}_{N,M}$  (Eqn. 7) with a predefined small number of clusters  $M$  (e.g.,  $M = 49$ ). Then,  $M$  latent tokens,  $Z_{M,C}$  are formed via simple matrix multiplication between the clustering assignment  $\mathcal{C}_{N,M}^T$  (transposed) and  $X_{N,C}$ . In inference, we can directly visualize the clusters  $\mathcal{C}_{N,M}$  as heatmaps to reveal what has been captured by the trained models (Fig. 4). The proposed PaCa module provides a way of jointly learning clustering-for-attention and attention-for-clustering in ViT models.

In experiments, the proposed PaCa-ViT model is tested on CIFAR-100 [25] and ImageNet-1000 [11] image classification, and MS-COCO object detection and instance segmentation [26]. Compared with prior arts, it obtains better performance in classification and comparable performance in detection and segmentation. The learned clusters are also semantically meaningful and shed light on designing more discriminative yet interpretable ViT models.

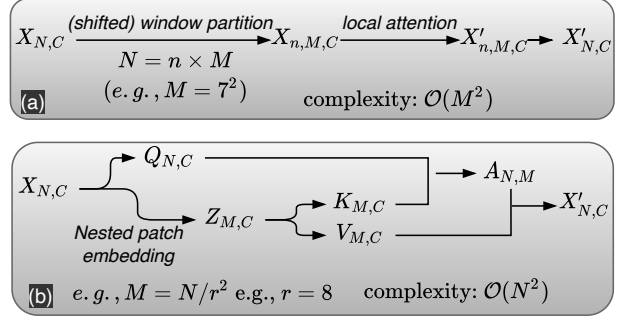


Figure 2. Two popular designs of reducing the complexity of the vanilla ViT models in vision applications (Fig. 1): (a) the shifted window based local attention and (b) patch embedding at a coarser level for computing keys/values respectively.

## 2. Related Work and Our Contributions

Since the pioneering work of ViT [12], there has already been a vast body of work leveraging and developing the Transformer model [40] that dominates the NLP field in computer vision [20]. We briefly review the efforts on addressing the quadratic complexity and the explanation of the ViT models.

**Efficient Transformer models.** There has been rapid progress in developing efficient Transformer models. [37] provides an excellent survey of different efforts in the literature. One family of approaches is to leverage inductive bias back in the Transformer, including the local window partition based methods [2, 4, 8, 27, 31] and random sparse patterns [54]. Although both computational and model performance can be improved, these models achieve them at the expense of limiting the capacity of a self-attention layer due to the locality constraints. Also, sophisticated designs are needed such as the shifted window and the masked attention method in the Swin-Transformer [27] (Fig. 2 (a)). The quad-tree based aggregating method proposed in the Nest [57] shows another promising direction. Another family of approaches exploits low-rank projections to form a coarser-grained representation of the input sequence, which have shown successful applications for certain NLP tasks such as the LinFormer [42], Nyströmformer [50] and Synthesizer [36]. Even though these methods retain the capability of enabling each token to attend to the entire input sequence, they suffer from the loss of high-fidelity token-wise information, and on tasks that require fine-grained local information, their performance can fall short of full attention or the aforementioned sparse attention. The proposed PaCa-ViT is motivated by addressing the redundancy of patches in patch-to-patch attention in computer vision applications, and shares the spirit of low-rank projection based efficient Transformer models.

**Transformer model explanation.** Driven by XAI [18]

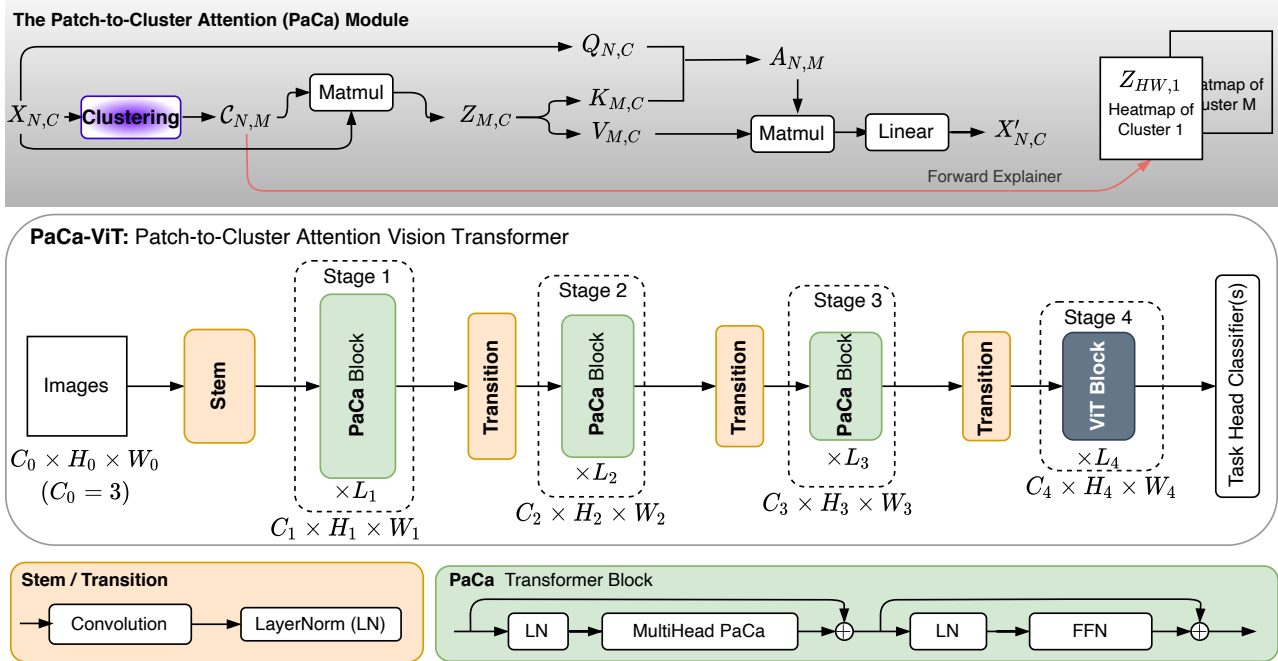


Figure 3. Illustration of the proposed ViT model, PaCa-ViT. It consists of a number of stages (e.g., 4), each of which has a number,  $L_i$  of the proposed PaCa variant of the vanilla Transformer blocks. The proposed PaCa variant of the vanilla Transformer block exploits the PaCa module in the multi-head self-attention. The FFN refers to the feed-forward network. The Stem and Transition module are implemented by a convolution module followed by the Layer Normalization (LN) [3]. ‘Matmul’ refers to the matrix multiplication operation.

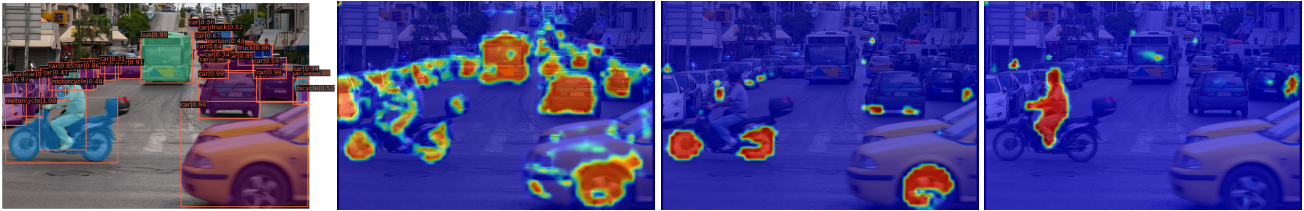


Figure 4. Examples of learned semantically meaningful clusters in the proposed PaCa module. The left-most image shows the detection and semantic segmentation results for an image in the COCO 2017 validation dataset ( $800 \times 1216$ ). The remaining three images show the heatmaps for three clusters which capture some semantically meaningful visual patterns in the image such as the person, the wheel and the vehicle respectively. See Sec. 3.5 for details.

and the natural curiosity of humanity, it is always desirable to understand what is going on inside big models like convolutional neural networks and Transformer models. For high-stake applications such as autonomous driving and medical healthcare diagnosis, the explainability is a must before deployment. There are mainly two categories of approaches: gradient based methods such as the GradCAM method [34] that is built on the CAM [59] and attribution based methods built on the deep Taylor decomposition framework [30] such as the Layerwise Relevance Propagation (LRP) method [5]. Both have achieved remarkable progress in explaining convolutional neural networks. The former can be computed in a class-specific way, but is of-

ten based only on the gradients of the deepest layers of a network, resulting in coarse heatmap visualization due to upsampling. The latter often has more assumptions of the non-linearity layers (e.g., ReLU) in order to compute the layerwise propagation properly. In addition to the two main schema, there are also some more direct methods including saliency based approaches [10, 29, 35, 55, 58, 59], activation maximization [14], excitation backpropagation [56], perturbation based approaches [15, 16], and the shapley-value based methods [28].

Most of the efforts have been focused on convolutional neural networks. Due to the remarkable progress made by the ViT model [12] and its variants, much attention has been

attracted to explaining ViT models, where many contributions employ the attention scores themselves. As pointed out in the Improved LRP [6], reducing the explanation to only the attentions scores may be myopic since many other components are ignored. Most of the efforts are also focused on the full attention ViT models. For pyramidal model configurations [27, 43, 44], it becomes less clear on how to interpret and visualize the attention scores due to the reduced granularity of the Key used in computing the attention matrix. The proposed patch-to-cluster attention remedies this due to the clustering component, which provides a forward explainer. This is complementary to existing approaches.

**Our Contributions.** This paper makes two main contributions for developing efficient Transformer models that enjoy forward explainability in computer vision applications: (i) It proposes a Patch-to-Cluster Attention (PaCa) module that paves the way of facilitating a conceptual shift of learning “visual tokens” beyond patches in ViT models. It also addresses the quadratic complexity of vanilla patch-to-patch attention and can account for the spatial redundancy of patches in the patch-to-patch attention. (ii) The proposed PaCa module enables a forward explainer for interpreting the trained models based on the learned semantically meaningful clusters. This provides an alternative to the existing post-hoc explanation methods in the XAI literature.

### 3. Approach

In this section, we first give an overview of the patch-to-patch multi-head self-attention, the vanilla Transformer block, and the stage-wise pyramid-like vision Transformer architecture to be self-contained. Then, we present details of the proposed patch-to-cluster (PaCa) module and the resulting PaCa-ViT models.

#### 3.1. Multi-Head Patch-to-Patch Self-Attention

Denote by  $\Lambda$  an image lattice of  $H_0 \times W_0$  pixels and by  $I_\Lambda$  a RGB image defined on the lattice. The image is first evenly chunked into  $N$  non-overlapping (typically square) patches of a predefined patch length  $p$  (e.g., 16). Without loss of generality, denote  $H = H_0/p, W = W_0/p$  and  $N = H \times W$ . The patches are embedded / encoded into a  $C$ -dim vector, resulting in the patch-based sequence  $X_{N,C}$ , or equivalently represented as the feature map  $X_{H,W,C}$ . For simplicity, we use the sequence terminology with the notation  $X_{N,C}$  in this paper. The  $N$  elements are also called patch tokens. Positional encoding can also be added to counter the permutation insensitivity of the self-attention computation [12, 40].

The input sequence  $X_{N,C}$  is first transformed via linear mapping into the Query/Key/Value sequence, denoted by  $Q_{N,C}, K_{N,C}$  and  $V_{N,C}$  respectively, as illustrated in Fig. 1.

The scaled dot-product attention is to compute the full pairwise attention matrix,

$$A_{N,N} = \text{Softmax}\left(\frac{Q_{N,C} \cdot K_{N,C}^T}{\sqrt{C}}\right)_{dim=1}, \quad (1)$$

where the Softmax is applied for each row as indicated by the subscript  $dim = 1$ . Both the computation and memory footprint have the complexity of  $\mathcal{O}(N^2)$ , i.e., quadratic in terms of the length of an input sequence.

Then, the output is computed by a simple matrix multiplication,  $X'_{N,C} = A_{N,N} \cdot V_{N,C}$ . By doing so, the input  $X_{N,C}$  first goes through a spatially-shared (i.e., channel-wise) linear transformation to the Value  $V_{N,C}$ , and then a depth-wise transformation using the learned attention matrix.

The Multi-head Self-Attention (MHSA) captures the patch-to-patch attention in different sub-spaces. It first chunks the Query/Key/Value sequence into a small number of heads,  $h$ , along the channel dimension. This result is  $Q_{h,N,d}, K_{h,N,d}$  and  $V_{h,N,d}$ , where  $h \times d = C$ . Then, the computed attention matrix is  $A_{N,N}^{(i)}$  and the output is  $X_{N,d}^{(i)}$  for each head  $i$ . The final output is then concatenated from  $X_{N,d}^{(i)}$ 's, followed by a linear transformation to fuse information between different heads.

The Transformer block consists of a MHSA component and a feed-forward network (FFN) with skip connections [23] and layer normalizations [3] used. The FFN often uses one hidden layer multi-layer perceptron (MLP). The full Transformer block can be defined by,

$$Z = X + \text{MHSA}(\text{LayerNorm}(X)), \quad (2)$$

$$X' = Z + \text{FFN}(\text{LayerNorm}(Z)) \quad (3)$$

In the ViT model, the Transformer block is applied in an isotropic way, that is the length of the sequence and the embedding dimension are kept the same throughout the network after computing the patch tokens. So, large patches are often used in practice to control the length of sequence. A high embedding dimension is also entailed to ensure the model capacity, resulting in large models and high strain on the computing resources for training such models.

#### 3.2. Stage-wise Architectures of ViT

To apply the Transformer block in a non-isotropic way and to resemble the conventional stage-wise building-block based schema of convolutional neural networks such as the ResNets [23], stage-wise architectures of ViT variants have been developed, which reduce the spatial dimensions in a pyramidal way while increasing the embedding dimensions. By doing so, smaller patches can be used in early stages and more model parameters can be devoted to later stages. But, the quadratic complexity of the vanilla MHSA needs to be

addressed for leveraging smaller patches. Overall, stage-wise architectures share the same scheme shown in Fig. 3 with different realizations of the Transformer blocks.

One straightforward way is to make the computation of MHSA (Eqn. 1) independent of the length  $N$  of an input sequence (see Fig. 2 (a)), which leads to the clever development of local attention methods such as the Swin-Transformer [27] and the Nested Transformer [57], which both obtain linear complexity.

Alternatively, we can rethink the realization of the MHSA. More specifically, the role of a query, key and value can be treated differently: The Query  $Q_{N,C}$  should be kept unchanged as to retain the full resolution of the input. The Key and Value need to be consistently “packed”, but are not necessarily required to retain the full sequence length. As shown in Fig. 2 (b), one key question is how to reduce the sequence length from  $N$  to a more manageable one,  $M$ , before computing the Key and the Value. To that end, another nested patch embedding is exploited as done in the latest PVTv2 [43]. Given a predefined patch size  $p_i$  at a stage  $i$ , we have,

$$Z_{M,C}^{pvt} = \text{LayerNorm}(\text{Conv2d}(X_{N,C}; k = p_i, s = p_i)), \quad (4)$$

where  $X_{N,C}$  is rearranged to  $X_{H,W,C}$  when applying the convolution with the kernel size  $p_i$  and the stride  $p_i$ . The resulting sequence length is  $M = N/p_i^2$ . **This approach does not prevent quadratic complexity, but rather reduces it by a ratio corresponding to the patch size.**

So, Eqn. (1) can be rewritten in a more general form,

$$A_{N,M} = \text{Softmax}\left(\frac{Q_{N,C} \cdot K_{M,C}^T}{\sqrt{C}}\right)_{dim=1}, \quad (5)$$

where the subscript  $dim = 1$  indicates that the Softmax is applied for each row.

Meanwhile, the MLP based FFN in the Transformer block has been substituted by the inverted bottleneck block proposed in the MobileNets-v2 [33], termed MBlock which utilizes a depth-wise convolution for the hidden layer. And, the non-overlapping patch embedding has been replaced by overlapping ones. With these modifications, positional encodings are not used in the network, partially due to the implicit position encoding capability of the zero-padding convolutions [24] used before (via the Stem and Transition module), inside (via the MBlock in the FFN) and after (via the Transition module) the modified Transformer block.

### 3.3. The Proposed Patch-to-Cluster Attention

To jointly enable reducing the length of the Key/Value and eliminate the potential obscuring of self-attention learning, we exploit the idea of clustering. One may think the nested patch embedding methods using strided convolution are performing locality-constrained clustering, but

due to the compositional nature of images and reusable parts/patterns in images, the locality-constrained clustering may not be sufficiently flexible to learn to cluster similar patterns that appear in various locations in an image. The nested patch embedding with adaptive average pooling may suffer from treating each element in a pooling window with equal importance, thus lacking the necessary adaptability and data-driven reweighing capability.

We propose a lightweight learnable clustering module to address the aforementioned issues, and the entire pipeline will still be end-to-end trainable. As shown in Fig. 3 (the bottom), given an input sequence  $X_{N,C}$  and a predefined number  $M$  of clusters, we first compute the cluster assignment  $Z_{N,M}$ . To put it another way, the goal is to segment the input sequence/feature map into  $M$  latent classes. More specifically, we choose to realize this by,

$$U_{N,c} = \text{GELU}(\text{Conv2d}(X_{N,C})), \quad (6)$$

$$C_{N,M} = \text{Softmax}(\text{Linear}(U_{N,c}))_{dim=0}, \quad (7)$$

where the first convolution module uses a  $3 \times 3$  kernel with stride 1 and zero padding 1, which is to integrate local information while squeezing the feature dimension from  $C$  to  $c$  with a predefined ratio  $r$  (e.g., 4),  $c = \frac{C}{r}$ . The squeezing operation is introduced with the attempt to force the input sequence  $X_{N,C}$  to be semantically meaningful in the sense that good clusters can be formed in the latent space of a lower feature dimension. The second linear transformation is to map the latent  $c$ -dim features to the  $M$  latent clusters.

To encourage forming meaningful clusters that can capture underlying visual patterns that are often spatially sparse, we apply Softmax along the spatial dimension (i.e.,  $dim = 0$ ) in Eqn. (7), which also enables directly visualizing  $C_{N,M}$  as  $M$  heatmaps as a means of diagnosing the interpretability of a trained model at the instance level in a forward computation (Fig. 4).

With the learned cluster assignment  $C_{N,M}$ , we can compute  $M$  visual tokens  $Z_{M,C}$  for the patch-to-cluster attention simply by,

$$Z_{M,C}^{paca} = \text{LayerNorm}(C_{N,M}^T \cdot X_{N,C}). \quad (8)$$

**Complexity Analyses.** Compared with Eqn. 4 used in PVTv2 [43], our PaCa (Eqn. 8) leads to *linear* complexity in computing the self-attention matrix (Eqn. 5) since the number of clusters  $M$  is predefined and fixed in our PaCa-ViT models. This advantage is achieved at the expense of the overhead cost in Eqn. 6, Eqn. 7 and the matrix multiplication in Eqn. 8. For relatively small images (e.g., in image classification), the overhead cost slightly outweighs the reduction in computing the self-attention matrix (see Sec. 4.1). For large images (e.g., in object detection and instance semantic segmentation), the overhead cost is well paid off, leading to significant reduction of computing cost and memory footprint (see Sec. 4.2).

### 3.4. Interpreting the Proposed PaCa Module

Intuitively, Eqn. 8 can be understood as a depth-wise global weighted pooling with learned weights. Eqn. 8 can also be seen as a dynamic MLP-Mixer [38] with data-driven weight parameters  $\mathcal{C}_{N,M}$  for the spatial transformation and integration component, rather than using top-down model parameters. So, it is more flexible without restricting the trained models to a specific input size. It is straightforward to compute the PaCa in a multi-head way. The overall multi-head PaCa based Transformer block is shown in Fig. 3, which provides a way of integrating a dynamic variant of MLP-Mixer and the MHSA.

Furthermore, the learned clustering assignment  $\mathcal{C}_{N,M}$  in Eqn. 7 has a similar spirit to and the same form of the attention matrix  $A_{N,M}$  in Eqn. 5. Eqn. 8 can thus be understood as performing cross-covariance attention (XCA) [13] too.

The clustering module in Eqn. 7 itself can be understood as a way of learning better visual tokens to bridge the gap between patches and the textual tokens used in natural language processing Transformer models. This type of visual tokenizer has also been observed to be useful in integrating Transformer models on top of convolution neural networks such as ResNets in Visual Transformer [46].

### 3.5. Network Interpretability via the PaCa Module

To select the most important clusters in  $\mathcal{C}_{N,M}$  (Eqn. 7) for an input image  $x$  in a vision task (e.g., image classification or object detection), we adopt a straightforward approach. For each cluster  $m$ , we reshape the slice  $\mathcal{C}_{N,m}$  back to a 2D spatial heatmap and normalize it (by subtracting the minimum and dividing the difference between the maximum and the minimum), denoted by  $\mathcal{H}_{h,w}^m$ . Then we compute the mask by  $1 - \mathcal{H}_{h,w}^m$  which is used to mask the input image (after being upsampled correspondingly). Denote the masked image by  $\tilde{x}^m$ . The importance of a cluster  $m$  is defined by the degradation of accuracy performance between  $x$  and  $\tilde{x}^m$ . The worse the performance  $\tilde{x}^m$  is, the more important the cluster  $m$  is. In other words, we treat the mask as an adversarial attack, and the stronger the attack is the more important the cluster is.

For image classification, let  $p_y(x)$  and  $p_y(\tilde{x}^m)$  be the softmax outputs for the images  $x$  and  $\tilde{x}^m$  with the ground-truth label  $y$ . We focus on images for which the trained model has correct prediction. Then, we use the difference  $(p_y(x) - p_y(\tilde{x}^m))$  as the figure of merits of the cluster  $m$ . If multiple clusters have similar effects, we select the one with minimum entropy indicating the cluster is the more precise in terms of contributing to the prediction. Similarly, for object detection and instance segmentation, we use as the figure of merit the difference of the mean average precision (AP) between the original image and the masked image. The aforementioned method can also be applied in visualizing the attention matrix  $A_{N,M}$  (Eqn. 5).

## 4. Experiment

In this section, we present experimental results of the proposed method in CIFAR-100 (C100) [25] and ImageNet-1000 (IN1K) [11] classification, and MS-COCO 2017 object detection and instance segmentation [26]. **Our PyTorch source code will be released.** In implementation, we use the popular `timm` PyTorch toolkit [45]. The pyramidal structure of the proposed PaCa-ViT is the same as PVTv2 [43]. Due to the limited computing resources, we do not explore and search for potentially better model configurations when accounting for the integration of PaCa module. For the same reason, we conduct experiments following the B0 to B2 settings used by PVTv2 [43] (Table. 1).

### 4.1. Image Classification

**ImageNet-1000** The ImageNet-1000 classification dataset [11] consists of about 1.28 million images for training, and 50,000 for validation, from 1,000 classes. All models are trained on the training set for fair comparison and report the Top-1 accuracy on the validation set using a single center crop. We follow the training recipe used by the PVTv2 which in turn is adopted from the DeiT [39].

**Accuracy.** Table 2 shows the comparison. The proposed PaCa-ViT obtains better performance than the baseline PVTv2. In terms of accuracy, it gains more for smaller model configurations. For bigger model (e.g., B2), the gain is less significant. One hypothesis is that the proposed PaCa-ViT may need different model configurations. For example, as shown in Table 1, both B0 and B1 use the same number of layers (2) per stage, while B2 uses a different configuration, (3,4,6,3). Due to the computing resource limit, we do not explore the tuning of those, but simply follow all hyper-parameters used in the baseline PVTv2.

**Efficiency.** In terms of efficiency based on the throughput (images/sec) shown in Table 2, as aforementioned, the proposed PaCa-ViT is inferior to the baseline PVTv2 due to the extra clustering component. However, our PaCa-ViT will be more efficient when image sizes are increased in testing. For example, if we use the resolution of  $384 \times 384$  in the ImageNet validation, the throughput of our PaCa-ViT-B2 is 428.4 images/sec, slightly faster than that of PVTv2-B2, 422.1 images/sec. The gain of efficiency will be more significant in downstream tasks with even larger input images (e.g., as can be observed in COCO, Table 4).

**Interpretability.** Fig. 5 and Fig. 6 shows some examples of visualizing the learned clusters in IN1K. The clusters are semantically meaningful (with some corresponding object parts) and show comparable or qualitatively better results to the state-of-the-art Improved LRP [6].

**CIFAR-100** The dataset consists of  $32 \times 32$  color images drawn from 100 classes [25]. The training and test sets contains 50,000 and 10,000 images respectively. It has been

	Output Size	Operation	PaCa-ViT		
			B0	B1	B2
Stage 1	$\frac{H_0}{s_1} \times \frac{W_0}{s_1}$ (e.g., $56 \times 56$ in IN1K, and $32 \times 32$ in C100)	Stem	$(k_1, s_1, p_1) = (7, 4, 3)/(3, 1, 1)$ in IN1K / C100 respectively $C_1 = 32$		
		MH-PaCa Block	#Clusters (Eqn. 7):		$M_1 = 49/64$
			Reduction ratio (Eqn. 6):		$r_1 = 4$
			#Heads:		$h_1 = 1$
			Expansion ratio in FFN (Eqn. 3):		$e_1 = 8$
			Depth: $L_1 = 2$		$L_1 = 3$
Stage 2	$\frac{H_0}{s_1 \times s_2} \times \frac{W_0}{s_1 \times s_2}$ (e.g., $28 \times 28$ in IN1K, and $16 \times 16$ in C100)	Transition	$(k_2, s_2, p_2) = (3, 2, 1)$ $C_2 = 64$		
		MH-PaCa Block	#Clusters (Eqn. 7):		$M_2 = 49/64$
			Reduction ratio (Eqn. 6):		$r_2 = 4$
			#Heads:		$h_2 = 2$
			Expansion ratio in FFN (Eqn. 3):		$e_2 = 8$
			Depth: $L_2 = 2$		$L_2 = 4$
Stage 3	$\frac{H_0}{s_1 \times s_2 \times s_3} \times \frac{W_0}{s_1 \times s_2 \times s_3}$ (e.g., $14 \times 14$ in IN1K, and $8 \times 8$ in C100)	Transition	$(k_3, s_3, p_3) = (3, 2, 1)$ $C_3 = 160$		
		MH-PaCa (in IN1K) / MHSA (in C100) Block	#Clusters (Eqn. 7):		$M_3 = 49/0$
			Reduction ratio (Eqn. 6):		$r_3 = 4$
			#Heads:		$h_3 = 5$
			Expansion ratio in FFN (Eqn. 3):		$e_3 = 4$
			Depth: $L_3 = 2$		$L_3 = 6$
Stage 4	$\frac{H_0}{s_1 \times s_2 \times s_3 \times s_4} \times \frac{W_0}{s_1 \times s_2 \times s_3 \times s_4}$ (e.g., $7 \times 7$ in IN1K, and $8 \times 8$ in C100)	Transition	$(k_4, s_4, p_4) = (3, 2, 1)/(3, 1, 1)$ $C_4 = 256$		
		MHSA Block	#Heads:		$h_4 = 8$
			Expansion ratio in FFN (Eqn. 3):		$e_4 = 4$
			Depth: $L_4 = 2$		$L_4 = 3$
			LayerNorm		
			Task head(s)		

Table 1. Network specifications of our PaCa-ViT (see Fig. 3) used in experiments.

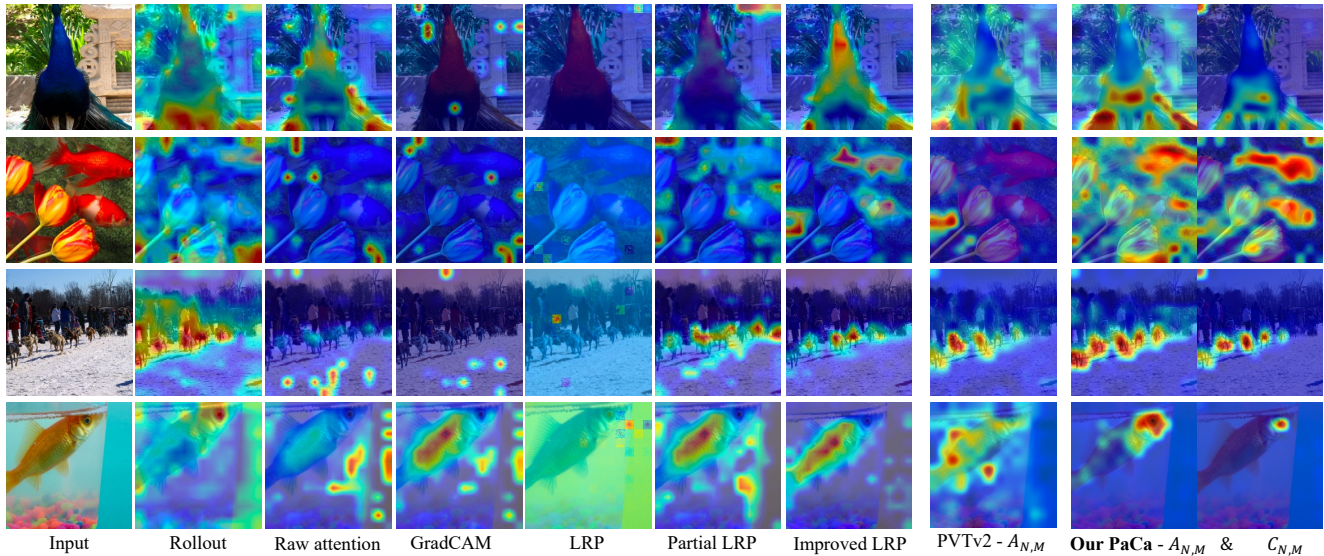


Figure 5. Visualization examples. Results of Rollout [1], raw attention, GradCAM [34], LRP [5], partial LRP [41] and the Improved LRP [6] are reproduced from [6], which all use the pretrained ViT-B model [12]. As done in Fig. 6, PVTv2 shows the top-1 attention matrix, and our PaCa shows the top-1 attention and cluster using the method presented in Sec. 3.5. Both are based on the ImageNet trained B2 models.

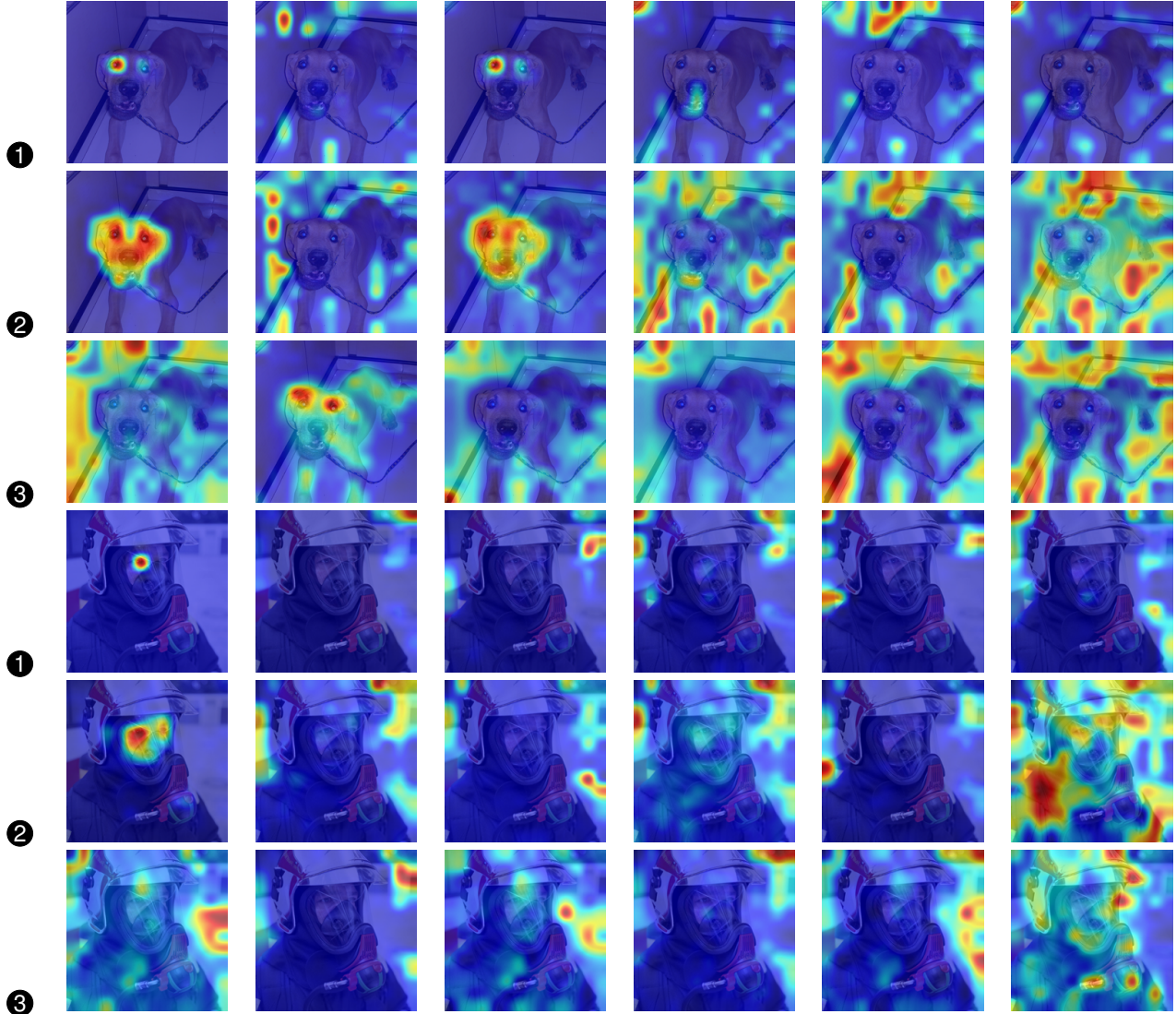


Figure 6. Visualizing the learned top-6 clusters in  $C_{N,M}$  of our PaCa in Eqn. 7 (shown with ❶), and top-6 channels in the attention matrix  $A_{N,M}$  in Eqn. 5 (shown with ❷ for our PaCa, and with ❸ for PVTv2). We can see that the proposed PaCa module can learn more localized “parts” on objects of interest, which are semantically meaningful.

shown that prior arts of Transformer based methods often do not perform well for small datasets such as CIFAR-100. We follow the training recipe used in the Nested Transformer [57].

Table 3 shows the comparisons. Both the baseline PVTv2 models and our proposed PaCa-ViT models work significantly better than prior arts. Our PaCa-ViT models outperform the baseline PVTv2. The integration of Transformer blocks and convolution (in Stem/Transition) in the PVTv2 scheme seems to have a strong positive effect on addressing the data efficiency issue of the counterpart. The improvement by the proposed PaCa-ViT shows that the patch-to-cluster attention is effective, compared to

the nested patch embedding methods in the baseline methods, PVTv2 and NesT. Furthermore, we modify the baseline PVTv2 using only pure vanilla MHSA since the complexity is not a big issue for the relatively small input ( $32 \times 32$ ) in C100. Overall, they are comparable to the vanilla baseline PVTv2. The results further suggest that patch-to-patch attention may not be needed due to the information redundancy caused by the reusable parts in images. The proposed patch-to-cluster attention can eliminate this to some extent with performance improved. In terms of efficiency, we have the same observation as the experiments in IN1K.



Method	#Params	Throughput	Top-1 Acc. (%)
PVTv2-B0 [43]	3.7M	1308.7	70.5
<b>PaCa-ViT-B0 (ours)</b>	3.4M	1241.5	<b>71.85</b> $\uparrow 1.35$
ResNet-18 [23]	11.7M	-	69.8
DeiT-T/16 [39]	5.7M	-	72.2
PVT-T [44]	13.2M	-	75.1
PVTv2-B1 [43]	14.0M	973.9	78.7
<b>PaCa-ViT-B1 (ours)</b>	12.7M	928.0	<b>79.47</b> $\uparrow 0.77$
ResNet-50 [23]	25.6M	-	76.1
ResNeXt-50-32x4d [49]	25.0M	-	77.6
RegNetY-4G [32]	21.0M	-	80.0
DeiT-S/16 [39]	22.1M	-	79.9
T2T-ViT <sub>r</sub> -14	22.0M	-	80.7
PVT-S [44]	24.5M	-	79.8
TNT-S [52]	23.8M	-	81.3
Swin-T [27]	29.0M	-	81.3
CvT-13 [47]	20.0M	-	81.6
CoaT-Lite-S [51]	20.0M	-	81.9
Twins-SVT-S [9]	24.0M	-	81.3
PVTv2-B2 [43]	25.4M	604.9	82.0
<b>PaCa-ViT-B2 (ours)</b>	22.7M	573.3	<b>82.28</b> $\uparrow 0.28$

Table 2. Top-1 accuracy comparison in IN1K validation set using the single center crop ( $224 \times 224$ ) evaluation protocol. Throughput (images/second) is computed on a single GPU (RTX 8000) with mixed precision (i.e., amp in PyTorch) using the `timm benchmark script` [45].

Model	Method	#Params	Throughput	Top-1 Acc. (%)
ConvNet	Pyramid-164-48 [19]	1.7M	3715.9	80.7
	WRN28-10 [53]	36.5M	1510.8	80.75
Transformer (local attention)	Swin-T [27]	27.5M	2399.2	78.07
	Swin-S [27]	48.8M	1372.5	77.01
	Swin-B [27]	86.7M	868.3	78.45
	NesT-T [57]	6.2M	1616.9	78.69
	NesT-S [57]	23.4M	627.9	81.70
	NesT-B [57]	90.1M	189.8	82.56
Transformer (full attention)	DeiT-T [39]	5.3M	1905.3	67.52
	DeiT-S [39]	21.3M	734.7	69.78
	DeiT-B [39]	85.1M	233.7	70.49
	CCT-7/3 $\times$ 1 [21]	3.7M	3040.2	76.67
	PVT-T [44]	12.8M	1478.1	69.62
	PVT-S [44]	24.1M	707.2	69.79
	PVT-B [44]	60.9M	315.1	43.78
	PVTv2-B0-pure	3.0M	2330.6	79.52
	PVTv2-B0 [43]	3.0M	3573.1	79.31
	<b>PaCa-ViT-B0 (ours)</b>	3.0M	3322.9	<b>79.58</b>
	PVTv2-B1-pure	11.7M	1495.8	82.26
	PVTv2-B1 [43]	11.9M	1977.1	82.51
	<b>PaCa-ViT-B1 (ours)</b>	11.8M	1859.3	<b>82.96</b>
PVTv2-B2-pure	20.6M	894.9	83.64	
PVTv2-B2 [43]	21.1M	1154.4	83.77	
<b>PaCa-ViT-B2 (ours)</b>	20.8M	1073.8	<b>84.18</b>	

Table 3. Top-1 accuracy comparison in C100. PVTv2 [43] and the proposed PaCa-ViT are trained from scratch following the same training recipe in the NesT [57], and other results are from the NesT paper [57]. PVTv2-b0/1/2-pure are models using the vanilla Transformer block (pure full attention).

## 4.2. Object Detection and Instance Segmentation

The challenging MS COCO-2017 benchmark [26] is used, which consists of a subset of train2017 (118k images) and a subset of val2017 (5k images). Following the

common settings, we use the IN1K pretrained PaCa-PVT models as the feature backbone, and test them using the Mask R-CNN framework [22]. The mmdetection PyTorch toolkit [7] is used.

**Accuracy and Efficiency.** Table 4 shows the comparison. The proposed PaCa-ViT obtains comparable performance with the baseline PVTv2, while being significantly more efficient as shown by the FLOPs and the peak GPU memory consumption in training.

**Interpretability.** The proposed PaCa-ViT can learn meaningful clusters as shown in Fig. 7. It is interesting to note that object parts seem to emerge in the clustering. For example, the person legs and the elephant legs in Fig. 7. Again, an automatic selection method is entailed, which needs to handle the more complicated operations such as the RoIAlign used in Mask RCNN and will be studied in the future work. It will also be interesting to study how to leverage this capability for object part discovery.

## 5. Conclusion

This paper studies a patch-to-cluster attention (PaCa) method in applying ViT models for computer vision tasks. The proposed PaCa can address the quadratic complexity issue and account for the spatial redundancy of patches in the commonly used patch-to-patch attention. It also provides a forward explainer for diagnosing the explainability of ViT models. A simple learnable clustering module is introduced for easy integration in the ViT models. In experiments, the proposed PaCa is tested in CIFAR-100 and ImageNet-1000 image classification and in the MS-COCO object detection and instance segmentation. It obtains better performance in classification, and comparable performance in detection and segmentation. It shows promising qualitative results of the learned clusters.

## Acknowledgements

R. Grainger, T. Paniagua and T. Wu were supported in part by NSF IIS-1909644, ARO Grant W911NF1810295, ARO Grant W911NF2210010, NSF IIS-1822477, NSF CMMI-2024688, NSF IUSE-2013451 and DHHS-ACL Grant 90IFDV0017-01-00. The views presented in this paper are those of the authors and should not be interpreted as representing any funding agencies.

## References

- [1] Samira Abnar and Willem Zuidema. Quantifying attention flow in transformers. *arXiv preprint arXiv:2005.00928*, 2020. 7
- [2] Joshua Ainslie, Santiago Ontanon, Chris Alberti, Vaclav Cvicek, Zachary Fisher, Philip Pham, Anirudh Ravula, Sumit Sanghai, Qifan Wang, and Li Yang. Etc: Encoding long and structured inputs in transformers. *arXiv preprint arXiv:2004.08483*, 2020. 2

Backbone	Mask R-CNN 1× (12 epochs)								
	#P(M)	FLOP (G)	Peak Memory (GB/Img)	AP <sup>b</sup>	AP <sub>50</sub> <sup>b</sup>	AP <sub>75</sub> <sup>b</sup>	AP <sup>m</sup>	AP <sub>50</sub> <sup>m</sup>	AP <sub>75</sub> <sup>m</sup>
PVTv2-B0 [43]	23.5	196.0	4.15	<b>38.2</b>	60.5	40.7	<b>36.2</b>	57.8	38.6
PaCa-ViT-B0 (ours)	23.1	<b>182.8</b>	<b>1.85</b>	<b>38.2</b>	60.6	40.8	35.9	57.6	38.3
ResNet-18 [23]	31.2	-	-	36.9	57.1	40.0	33.6	53.9	35.7
PVT-T [44]	32.9	-	-	39.8	62.2	43.0	37.4	59.3	39.9
PVTv2-B1 [43]	33.7	243.7	5.17	<b>41.8</b>	64.3	45.9	<b>38.8</b>	61.2	41.6
PaCa-ViT-B1 (ours)	32.4	<b>218.2</b>	<b>2.62</b>	<b>41.8</b>	64.2	45.4	38.7	61.1	41.4
ResNet-50 [23]	44.2	-	-	41.0	61.7	44.9	37.1	58.4	40.1
PVT-S [44]	44.1	-	-	43.0	65.3	46.9	39.9	62.5	42.8
PVTv2-B2 [43]	45.0	309.2	8.03	<b>45.3</b>	67.1	49.6	<b>41.2</b>	64.2	44.4
PaCa-ViT-B2 (ours)	42.4	<b>261.5</b>	<b>3.93</b>	<b>45.3</b>	67.1	49.3	<b>41.2</b>	64.3	44.3

Table 4. Object detection and instance segmentation on COCO val2017 [26] using the IN1K pretrained backbones and the Mask R-CNN [22].

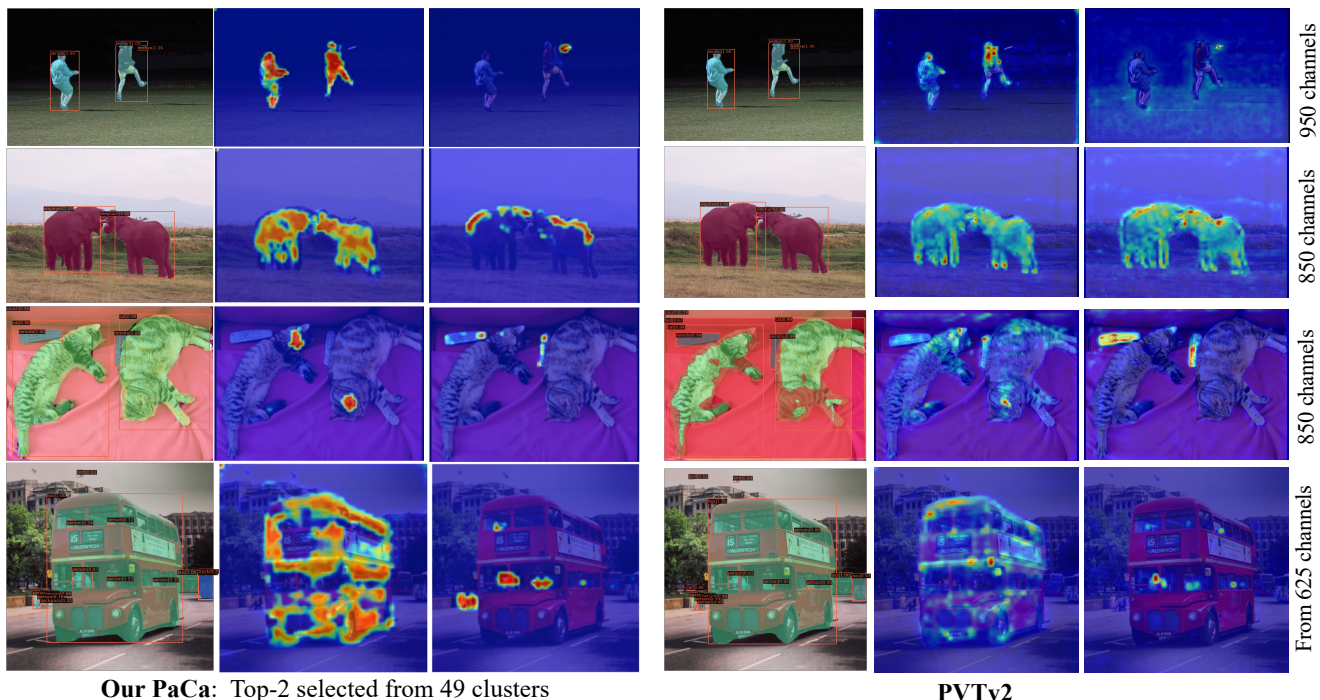


Figure 7. Visualization examples of learned clusters in our PaCa-ViT in COCO. The clusters are from the last clustering layer (layer 12) of PaCa-ViT-B2. For the PVTv2 results, since there are much more channels in their attention matrix (10x more than the number of clusters in our PaCa-ViT), the automatic selection of top-k channels does not work since there are attention channels that spread a major portion of the entire image and they will show up in the proposed automatic selection method. Instead, the two channels are manually selected which are most similar to the PaCa results. We can see the explaining PVTv2 entails much more efforts since they do not form compact “tokens” as our PaCa.

[3] Jimmy Lei Ba, Jamie Ryan Kiros, and Geoffrey E Hinton. Layer normalization. *arXiv preprint arXiv:1607.06450*, 2016. 3, 4

[4] Iz Beltagy, Matthew E Peters, and Arman Cohan. Longformer: The long-document transformer. *arXiv preprint arXiv:2004.05150*, 2020. 2

[5] Alexander Binder, Grégoire Montavon, Sebastian La-

puschkin, Klaus-Robert Müller, and Wojciech Samek. Layer-wise relevance propagation for neural networks with local renormalization layers. In *International Conference on Artificial Neural Networks*, pages 63–71. Springer, 2016. 3, 7

[6] Hila Chefer, Shir Gur, and Lior Wolf. Transformer interpretability beyond attention visualization. In *Proceedings of*

- the IEEE/CVF Conference on Computer Vision and Pattern Recognition*, pages 782–791, 2021. 1, 4, 6, 7
- [7] Kai Chen, Jiaqi Wang, Jiangmiao Pang, Yuhang Cao, Yu Xiong, Xiaoxiao Li, Shuyang Sun, Wansen Feng, Ziwei Liu, Jiarui Xu, et al. Mmdetection: Open mmlab detection toolbox and benchmark. *arXiv preprint arXiv:1906.07155*, 2019. 9
- [8] Rewon Child, Scott Gray, Alec Radford, and Ilya Sutskever. Generating long sequences with sparse transformers. *arXiv preprint arXiv:1904.10509*, 2019. 2
- [9] Xiangxiang Chu, Zhi Tian, Yuqing Wang, Bo Zhang, Haibing Ren, Xiaolin Wei, Huaxia Xia, and Chunhua Shen. Twins: Revisiting the design of spatial attention in vision transformers. *arXiv preprint arXiv:2104.13840*, 1(2):3, 2021. 9
- [10] Piotr Dabkowski and Yarin Gal. Real time image saliency for black box classifiers. *arXiv preprint arXiv:1705.07857*, 2017. 3
- [11] Jia Deng, Wei Dong, Richard Socher, Li-Jia Li, Kai Li, and Li Fei-Fei. Imagenet: A large-scale hierarchical image database. In *2009 IEEE conference on computer vision and pattern recognition*, pages 248–255. Ieee, 2009. 2, 6
- [12] Alexey Dosovitskiy, Lucas Beyer, Alexander Kolesnikov, Dirk Weissenborn, Xiaohua Zhai, Thomas Unterthiner, Mostafa Dehghani, Matthias Minderer, Georg Heigold, Sylvain Gelly, et al. An image is worth 16x16 words: Transformers for image recognition at scale. *arXiv preprint arXiv:2010.11929*, 2020. 1, 2, 3, 4, 7
- [13] Alaaeldin El-Nouby, Hugo Touvron, Mathilde Caron, Piotr Bojanowski, Matthijs Douze, Armand Joulin, Ivan Laptev, Natalia Neverova, Gabriel Synnaeve, Jakob Verbeek, et al. Xcit: Cross-covariance image transformers. *arXiv preprint arXiv:2106.09681*, 2021. 6
- [14] Dumitru Erhan, Yoshua Bengio, Aaron Courville, and Pascal Vincent. Visualizing higher-layer features of a deep network. *University of Montreal*, 1341(3):1, 2009. 3
- [15] Ruth Fong, Mandela Patrick, and Andrea Vedaldi. Understanding deep networks via extremal perturbations and smooth masks. In *Proceedings of the IEEE/CVF International Conference on Computer Vision*, pages 2950–2958, 2019. 3
- [16] Ruth C Fong and Andrea Vedaldi. Interpretable explanations of black boxes by meaningful perturbation. In *Proceedings of the IEEE international conference on computer vision*, pages 3429–3437, 2017. 3
- [17] Stuart Geman, Daniel Potter, and Zhi Yi Chi. Composition systems. *Quarterly of Applied Mathematics*, 60(4):707–736, 2002. 2
- [18] David Gunning, Mark Stefik, Jaesik Choi, Timothy Miller, Simone Stumpf, and Guang-Zhong Yang. Xai—explainable artificial intelligence. *Science Robotics*, 4(37), 2019. 1, 2
- [19] Dongyoon Han, Jiwhan Kim, and Junmo Kim. Deep pyramidal residual networks. In *Proceedings of the IEEE conference on computer vision and pattern recognition*, pages 5927–5935, 2017. 9
- [20] Kai Han, Yunhe Wang, Hanting Chen, Xinghao Chen, Jianyuan Guo, Zhenhua Liu, Yehui Tang, An Xiao, Chungjing Xu, Yixing Xu, et al. A survey on visual transformer. *arXiv preprint arXiv:2012.12556*, 2020. 2
- [21] Ali Hassani, Steven Walton, Nikhil Shah, Abulikemu Abuduweili, Jiachen Li, and Humphrey Shi. Escaping the big data paradigm with compact transformers. *arXiv preprint arXiv:2104.05704*, 2021. 9
- [22] Kaiming He, Georgia Gkioxari, Piotr Dollár, and Ross Girshick. Mask r-cnn. In *Proceedings of the IEEE international conference on computer vision*, pages 2961–2969, 2017. 9, 10
- [23] Kaiming He, Xiangyu Zhang, Shaoqing Ren, and Jian Sun. Deep residual learning for image recognition. In *Proceedings of the IEEE conference on computer vision and pattern recognition*, pages 770–778, 2016. 4, 9, 10
- [24] Md Amirul Islam, Sen Jia, and Neil DB Bruce. How much position information do convolutional neural networks encode? *arXiv preprint arXiv:2001.08248*, 2020. 5
- [25] Alex Krizhevsky, Geoffrey Hinton, et al. Learning multiple layers of features from tiny images. 2009. 2, 6
- [26] Tsung-Yi Lin, Michael Maire, Serge Belongie, James Hays, Pietro Perona, Deva Ramanan, Piotr Dollár, and C Lawrence Zitnick. Microsoft coco: Common objects in context. In *European conference on computer vision*, pages 740–755. Springer, 2014. 2, 6, 9, 10
- [27] Ze Liu, Yutong Lin, Yue Cao, Han Hu, Yixuan Wei, Zheng Zhang, Stephen Lin, and Baining Guo. Swin transformer: Hierarchical vision transformer using shifted windows. *arXiv preprint arXiv:2103.14030*, 2021. 1, 2, 4, 5, 9
- [28] Scott M Lundberg and Su-In Lee. A unified approach to interpreting model predictions. In *Proceedings of the 31st international conference on neural information processing systems*, pages 4768–4777, 2017. 3
- [29] Aravindh Mahendran and Andrea Vedaldi. Visualizing deep convolutional neural networks using natural pre-images. *International Journal of Computer Vision*, 120(3):233–255, 2016. 3
- [30] Grégoire Montavon, Sebastian Lapuschkin, Alexander Binder, Wojciech Samek, and Klaus-Robert Müller. Explaining nonlinear classification decisions with deep taylor decomposition. *Pattern Recognition*, 65:211–222, 2017. 3
- [31] Niki Parmar, Ashish Vaswani, Jakob Uszkoreit, Lukasz Kaiser, Noam Shazeer, Alexander Ku, and Dustin Tran. Image transformer. In *International Conference on Machine Learning*, pages 4055–4064. PMLR, 2018. 2
- [32] Ilija Radosavovic, Raj Prateek Kosaraju, Ross Girshick, Kaiming He, and Piotr Dollár. Designing network design spaces. In *Proceedings of the IEEE/CVF Conference on Computer Vision and Pattern Recognition*, pages 10428–10436, 2020. 9
- [33] Mark Sandler, Andrew Howard, Menglong Zhu, Andrey Zhmoginov, and Liang-Chieh Chen. Mobilenetv2: Inverted residuals and linear bottlenecks. In *Proceedings of the IEEE conference on computer vision and pattern recognition*, pages 4510–4520, 2018. 5
- [34] Ramprasaath R Selvaraju, Michael Cogswell, Abhishek Das, Ramakrishna Vedantam, Devi Parikh, and Dhruv Batra.

- Grad-cam: Visual explanations from deep networks via gradient-based localization. In *Proceedings of the IEEE international conference on computer vision*, pages 618–626, 2017. 3, 7
- [35] Karen Simonyan, Andrea Vedaldi, and Andrew Zisserman. Deep inside convolutional networks: Visualising image classification models and saliency maps. *arXiv preprint arXiv:1312.6034*, 2013. 3
- [36] Y Tay, D Bahri, D Metzler, D Juan, Z Zhao, and C Zheng. Synthesizer: Rethinking self-attention in transformer models. arxiv 2020. *arXiv preprint arXiv:2005.00743*, 2020. 2
- [37] Yi Tay, Mostafa Dehghani, Dara Bahri, and Donald Metzler. Efficient transformers: A survey. *arXiv preprint arXiv:2009.06732*, 2020. 2
- [38] Ilya Tolstikhin, Neil Houlsby, Alexander Kolesnikov, Lucas Beyer, Xiaohua Zhai, Thomas Unterthiner, Jessica Yung, Andreas Steiner, Daniel Keysers, Jakob Uszkoreit, et al. Mlp-mixer: An all-mlp architecture for vision. *arXiv preprint arXiv:2105.01601*, 2021. 6
- [39] Hugo Touvron, Matthieu Cord, Matthijs Douze, Francisco Massa, Alexandre Sablayrolles, and Hervé Jégou. Training data-efficient image transformers & distillation through attention. In *International Conference on Machine Learning*, pages 10347–10357. PMLR, 2021. 6, 9
- [40] Ashish Vaswani, Noam Shazeer, Niki Parmar, Jakob Uszkoreit, Llion Jones, Aidan N Gomez, Łukasz Kaiser, and Illia Polosukhin. Attention is all you need. In *Advances in neural information processing systems*, pages 5998–6008, 2017. 1, 2, 4
- [41] Elena Voita, David Talbot, Fedor Moiseev, Rico Sennrich, and Ivan Titov. Analyzing multi-head self-attention: Specialized heads do the heavy lifting, the rest can be pruned. *arXiv preprint arXiv:1905.09418*, 2019. 7
- [42] Sinong Wang, Belinda Li, Madian Khabsa, Han Fang, and H Linformer Ma. Self-attention with linear complexity. *arXiv preprint arXiv:2006.04768*, 2020. 2
- [43] Wenhai Wang, Enze Xie, Xiang Li, Deng-Ping Fan, Kaitao Song, Ding Liang, Tong Lu, Ping Luo, and Ling Shao. Ptv2: Improved baselines with pyramid vision transformer, 2021. 1, 2, 4, 5, 6, 9, 10
- [44] Wenhai Wang, Enze Xie, Xiang Li, Deng-Ping Fan, Kaitao Song, Ding Liang, Tong Lu, Ping Luo, and Ling Shao. Pyramid vision transformer: A versatile backbone for dense prediction without convolutions, 2021. 1, 2, 4, 9, 10
- [45] Ross Wightman. Pytorch image models. <https://github.com/rwightman/pytorch-image-models>, 2019. 6, 9
- [46] Bichen Wu, Chenfeng Xu, Xiaoliang Dai, Alvin Wan, Peizhao Zhang, Zhicheng Yan, Masayoshi Tomizuka, Joseph Gonzalez, Kurt Keutzer, and Peter Vajda. Visual transformers: Token-based image representation and processing for computer vision. *arXiv preprint arXiv:2006.03677*, 2020. 6
- [47] Haiping Wu, Bin Xiao, Noel Codella, Mengchen Liu, Xiyang Dai, Lu Yuan, and Lei Zhang. Cvt: Introducing convolutions to vision transformers. *arXiv preprint arXiv:2103.15808*, 2021. 9
- [48] Yu-Huan Wu, Yun Liu, Xin Zhan, and Ming-Ming Cheng. P2t: Pyramid pooling transformer for scene understanding. *arXiv preprint arXiv:2106.12011*, 2021. 1
- [49] Saining Xie, Ross Girshick, Piotr Dollár, Zhuowen Tu, and Kaiming He. Aggregated residual transformations for deep neural networks. In *Proceedings of the IEEE conference on computer vision and pattern recognition*, pages 1492–1500, 2017. 9
- [50] Yuyang Xiong, Zhanpeng Zeng, Rudrasis Chakraborty, Mingxing Tan, Glenn Fung, Yin Li, and Vikas Singh. Nyströmformer: A nyström-based algorithm for approximating self-attention. *arXiv preprint arXiv:2102.03902*, 2021. 2
- [51] Weijian Xu, Yifan Xu, Tyler Chang, and Zhuowen Tu. Co-scale conv-attentional image transformers. *arXiv preprint arXiv:2104.06399*, 2021. 9
- [52] Li Yuan, Yunpeng Chen, Tao Wang, Weihao Yu, Yujun Shi, Zihang Jiang, Francis EH Tay, Jiashi Feng, and Shuicheng Yan. Tokens-to-token vit: Training vision transformers from scratch on imagenet. *arXiv preprint arXiv:2101.11986*, 2021. 9
- [53] Sergey Zagoruyko and Nikos Komodakis. Wide residual networks. *arXiv preprint arXiv:1605.07146*, 2016. 9
- [54] Manzil Zaheer, Guru Guruganesh, Kumar Avinava Dubey, Joshua Ainslie, Chris Alberti, Santiago Ontanon, Philip Pham, Anirudh Ravula, Qifan Wang, Li Yang, et al. Big bird: Transformers for longer sequences. In *NeurIPS*, 2020. 2
- [55] Matthew D Zeiler and Rob Fergus. Visualizing and understanding convolutional networks. In *European conference on computer vision*, pages 818–833. Springer, 2014. 3
- [56] Jianming Zhang, Sarah Adel Bargal, Zhe Lin, Jonathan Brandt, Xiaohui Shen, and Stan Sclaroff. Top-down neural attention by excitation backprop. *International Journal of Computer Vision*, 126(10):1084–1102, 2018. 3
- [57] Zizhao Zhang, Han Zhang, Long Zhao, Ting Chen, and Tomas Pfister. Aggregating nested transformers. *arXiv preprint arXiv:2105.12723*, 2021. 1, 2, 5, 8, 9
- [58] Bolei Zhou, David Bau, Aude Oliva, and Antonio Torralba. Interpreting deep visual representations via network dissection. *IEEE transactions on pattern analysis and machine intelligence*, 41(9):2131–2145, 2018. 3
- [59] Bolei Zhou, Aditya Khosla, Agata Lapedriza, Aude Oliva, and Antonio Torralba. Learning deep features for discriminative localization. In *Proceedings of the IEEE conference on computer vision and pattern recognition*, pages 2921–2929, 2016. 3